51. Plots of Cross Sections and Related Quantities

Updated in 2017. See various sections for details.

This section contains a compilation of plots and tables on cross sections and related quantities that are not covered by other reviews but may be of interest to the community. The topics include:

– Pseudorapidity distributions in pp and $\overline{p}p$ interactions

– Table of average hadron multiplicities in hadronic e^+e^- annihilation events

– Cross section and R ratio in e^+e^- collisions

– R ratio in light-flavor, charm, and beauty threshold regions

– Annihilation cross section near M_Z

– Total cross section plots for hadronic (e.g. pp and $\overline{p}p$ collisions), γp, γd, and $\gamma\gamma$ processes

Pseudorapidity Distributions in pp and $\overline{p}p$ Interactions

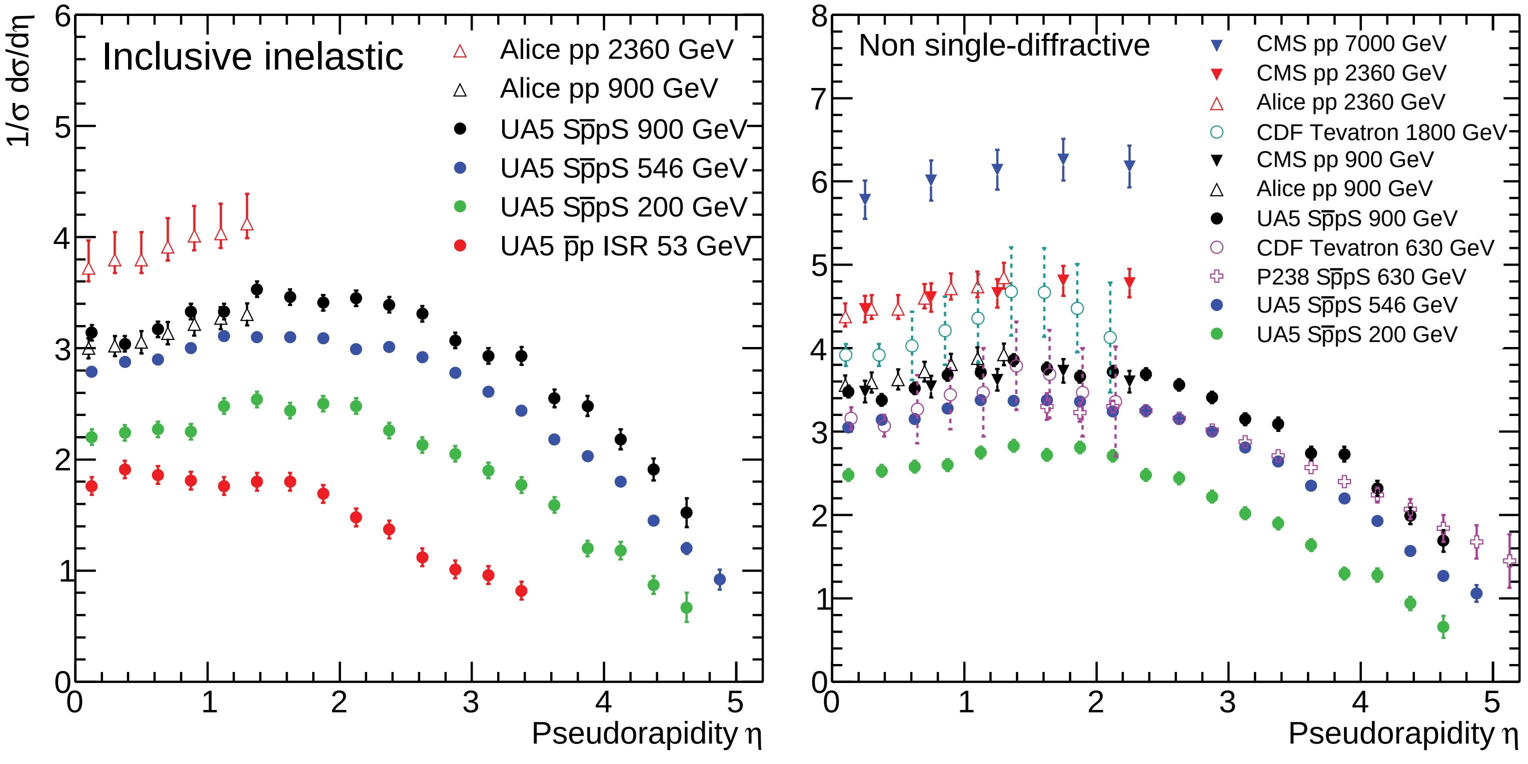

Figure 51.1: Charged particle pseudorapidity distributions in $p\overline{p}$ collisions for 53 GeV $\leq \sqrt{s} \leq$ 1800 GeV. UA5 data from the S$p\overline{p}$S are taken from G.J.Alner *et al.*, Z. Phys. **C33**, 1 (1986), and from the ISR from K.Alpgøard *et al.*, Phys.Lett. 112B 193 (1982). The UA5 data are shown for both the full inelastic cross-section and with singly diffractive events excluded. Additional non single-diffractive measurements are available from CDF at the Tevatron, F.Abe *et al.*, Phys. Rev. **D41**, 2330 (1990) and from P238 at the S$p\overline{p}$S, R.Harr *et al.*, Phys. Lett. **B401**, 176 (1997). These may be compared with both inclusive and non single-diffractive measurements in pp collisions at the LHC from ALICE, K.Aamodt *et al.*, Eur. Phys. J. **C68**, 89 (2010) and for non single-diffractive interactions from CMS , V.Khachatryan *et al.*, JHEP 1002:041 (2010), Phys. Rev. Lett. **105**, 022002 (2010). (Courtesy of D.R. Ward, Cambridge Univ., 2013)

Average Hadron Multiplicities in Hadronic e^+e^- Annihilation Events

Table 51.1: Average hadron multiplicities per hadronic e^+e^- annihilation event at $\sqrt{s} \approx 10$, 29–35, 91, and 130–200 GeV. The rates given include decay products from resonances with $c\tau < 10$ cm, and include the corresponding anti-particle state. Correlations of the systematic uncertainties were considered for the calculation of the averages. Quoted errors are not increased by scale factor S. (Updated August 2017 by O. Biebel, LMU, Munich)

Particle	$\sqrt{s} \approx 10$ GeV	$\sqrt{s} = 29$–35 GeV	$\sqrt{s} = 91$ GeV	$\sqrt{s} = 130$–200 GeV
Pseudoscalar mesons:				
π^+	6.52 ± 0.11	10.3 ± 0.4	17.02 ± 0.19	21.24 ± 0.39
π^0	3.2 ± 0.3	5.83 ± 0.28	9.42 ± 0.32	
K^+	0.953 ± 0.018	1.48 ± 0.09	2.228 ± 0.059	2.82 ± 0.19
K^0	0.91 ± 0.05	1.48 ± 0.07	2.049 ± 0.026	2.10 ± 0.12
η	0.20 ± 0.04	0.61 ± 0.07	1.049 ± 0.080	
$\eta\prime(958)$	0.03 ± 0.01	0.26 ± 0.10	0.152 ± 0.020	
D^+	$0.194 \pm 0.019^{(a)}$	0.17 ± 0.03	0.175 ± 0.016	
D^0	$0.446 \pm 0.032^{(a)}$	0.45 ± 0.07	0.454 ± 0.030	
D_s^+	$0.063 \pm 0.014^{(a)}$	$0.45 \pm 0.20^{(b)}$	0.131 ± 0.021	
$B^{(c)}$	—	—	$0.134 \pm 0.016^{(d)}$	
B^+	—	—	$0.141 \pm 0.004^{(d)}$	
B_s^0	—	—	$0.054 \pm 0.011^{(d)}$	
Scalar mesons:				
$f_0(980)$	0.024 ± 0.006	$0.05 \pm 0.02^{(e)}$	0.146 ± 0.012	
$a_0(980)^\pm$	—	—	$0.27 \pm 0.11^{(f)}$	
Vector mesons:				
$\rho(770)^0$	0.35 ± 0.04	0.81 ± 0.08	1.231 ± 0.098	
$\rho(770)^\pm$	—	—	$2.40 \pm 0.43^{(f)}$	
$\omega(782)$	0.30 ± 0.08	—	1.016 ± 0.065	
$K^*(892)^+$	0.27 ± 0.03	0.64 ± 0.05	0.714 ± 0.055	
$K^*(892)^0$	0.29 ± 0.03	0.56 ± 0.06	0.738 ± 0.024	
$\phi(1020)$	0.044 ± 0.003	0.085 ± 0.011	0.0963 ± 0.0032	
$D^*(2010)^+$	$0.177 \pm 0.022^{(a)}$	0.43 ± 0.07	$0.1937 \pm 0.0057^{(g)}$	
$D^*(2007)^0$	$0.168 \pm 0.019^{(a)}$	0.27 ± 0.11	—	
$D_s^*(2112)^+$	$0.048 \pm 0.014^{(a)}$	—	$0.101 \pm 0.048^{(h)}$	
$B^{*\ (i)}$	—	—	0.288 ± 0.026	
$J/\psi(1S)$	$0.00050 \pm 0.00005^{(a)}$	—	$0.0052 \pm 0.0004^{(j)}$	
$\psi(2S)$	—	—	$0.0023 \pm 0.0004^{(j)}$	
$\Upsilon(1S)$	—	—	$0.00014 \pm 0.00007^{(j)}$	
Pseudovector mesons:				
$f_1(1285)$	—	—	0.165 ± 0.051	
$f_1(1420)$	—	—	0.056 ± 0.012	
$\chi_{c1}(3510)$	—	—	$0.0041 \pm 0.0011^{(j)}$	
Tensor mesons:				
$f_2(1270)$	0.09 ± 0.02	0.14 ± 0.04	0.166 ± 0.020	
$f_2'(1525)$	—	—	0.012 ± 0.006	
$K_2^*(1430)^+$	—	0.09 ± 0.03	—	
$K_2^*(1430)^0$	—	0.12 ± 0.06	0.084 ± 0.022	
$B^{**\ (k)}$	—	—	0.118 ± 0.024	
$D_{s1}^\pm$	—	—	$0.0052 \pm 0.0011^{(\ell)}$	
$D_{s2}^{*\pm}$	—	—	$0.0083 \pm 0.0031^{(\ell)}$	
Baryons:				
p	0.266 ± 0.008	0.640 ± 0.050	1.050 ± 0.032	1.41 ± 0.18
Λ	$0.093 \pm 0.006^{(a)}$	0.205 ± 0.010	0.3915 ± 0.0065	0.39 ± 0.03
Σ^0	$0.0221 \pm 0.0018^{(a)}$	—	0.078 ± 0.010	
Σ^-	—	—	0.081 ± 0.010	
Σ^+	—	—	0.107 ± 0.011	
$\Sigma^\pm$	—	—	0.174 ± 0.009	
Ξ^-	$0.0055 \pm 0.0004^{(a)}$	0.0176 ± 0.0027	0.0262 ± 0.0009	
$\Delta(1232)^{++}$	0.040 ± 0.010	—	0.085 ± 0.014	
$\Sigma(1385)^-$	0.006 ± 0.002	0.017 ± 0.004	0.0240 ± 0.0017	
$\Sigma(1385)^+$	$0.0062 \pm 0.0011^{(a)}$	0.017 ± 0.004	0.0239 ± 0.0015	
$\Sigma(1385)^\pm$	0.0106 ± 0.0020	0.033 ± 0.008	0.0472 ± 0.0027	
$\Xi(1530)^0$	$0.00130 \pm 0.00010^{(a)}$	—	0.00694 ± 0.00049	
Ω^-	$0.00060 \pm 0.00033^{(a)}$	0.014 ± 0.007	0.00124 ± 0.00018	
Λ_c^+	$0.0479 \pm 0.0038^{(a,m)}$	0.110 ± 0.050	0.078 ± 0.017	
Λ_b^0	—	—	0.031 ± 0.016	
Σ_c^0	$0.0025 \pm 0.0004^{(a)}$	—	—	
$\Lambda(1520)$	$0.0046 \pm 0.0004^{(a)}$	—	0.0222 ± 0.0027	

Notes for Table 51.1:

(*a*) $\sigma_{\rm had} = 3.33 \pm 0.05 \pm 0.21$ nb (**CLEO**: Phys. Rev. **D29**, 1254 (1984)) has been used in converting the measured cross sections to average hadron multiplicities.

(*b*) $\mathrm{B}(D_s \to \eta\pi,\ \eta'\pi)$ was used (RPP 1994).

(*c*) Comprises both charged and neutral B meson states.

(*d*) The Standard Model $\mathrm{B}(Z \to b\overline{b}) = 0.217$ was used.

(*e*) $x_p = p/p_{\rm beam} > 0.1$ only.

(*f*) Both charge states.

(*g*) $\mathrm{B}(D^*(2010)^+ \to D^0\pi^+) \times \mathrm{B}(D^0 \to K^-\pi^+)$ has been used (RPP 2000).

(*h*) $\mathrm{B}(D_s^* \to D_S^+\gamma)$, $\mathrm{B}(D_s^+ \to \phi\pi^+)$, $\mathrm{B}(\phi \to K^+K^-)$ have been used (RPP 1998).

(*i*) Any charge state (*i.e.*, B_d^*, B_u^*, or B_s^*).

(*j*) $\mathrm{B}(Z \to \text{hadrons}) = 0.699$ was used (RPP 1994).

(*k*) Any charge state (*i.e.*, B_d^{**}, B_u^{**}, or B_s^{**}).

(*ℓ*) Assumes $\mathrm{B}(D_{s1}^+ \to D^{*+}K^0 + D^{*0}K+) = 100\%$ and $\mathrm{B}(D_{s2}^+ \to D^0K^+) = 45\%$.

(*m*) The value was derived from the cross section of $\Lambda_c^+ \to p\pi K$ using (*a*) and assuming the branching fraction to be $(5.0 \pm 1.3)\%$ (RPP 2004).

References for Table 51.1:

RPP 1992: Phys. Rev. **D45** (1992); **RPP 1994**: Phys. Rev. **D50**, 1173 (1994); **RPP 1996**: Phys. Rev. **D54**, 1 (1996); **RPP 1998**: Eur. Phys. J. **C3**, 1 (1998); **RPP 2000**: Eur. Phys. J. **C15**, 1 (2000); **RPP 2002**: Phys. Rev. **D66**, 010001 (2002); **RPP 2004**: Phys. Lett. **B592**, 1 (2004); **RPP 2006**: J. Phys. **G33**, 1 (2006); **RPP 2008**: Phys. Lett. **B667**, 1 (2008); **RPP 2010**: J. Phys. **G37**, 075021 (2010); **RPP 2012**: Phys. Rev. D 86,010001(2012) and references therein; **RPP 2014**: Chin. Phys. C **38**, 090001 (2014) and references therein; **RPP 2016**: Chin. Phys. C **40**, 100001 (2016) and references therein.

R. Marshall, Rept. on Prog. in Phys. **52**, 1329 (1989). A. De Angelis, J. Phys. **G19**, 1233 (1993) and references therein.

ALEPH: D. Buskulic *et al.*: Phys. Lett. **B295**, 396 (1992); Z. Phys. **C64**, 361 (1994); **C69**, 15 (1996); **C69**, 379 (1996); **C73**, 409 (1997); and R. Barate *et al.*: Z. Phys. **C74**, 451 (1997); Phys. Reports **294**, 1 (1998); Eur. Phys. J. **C5**, 205 (1998); **C16**, 597 (2000); **C16**, 613 (2000); and A. Heister *et al.*: Phys. Lett. **B526**, 34 (2002); **B528**, 19 (2002).

ARGUS: H. Albrecht *et al.*: Phys. Lett. **230B**, 169 (1989); Z. Phys. **C39**, 177 (1988); **C44**, 547 (1989); **C46**, 15 (1990); **C54**, 1 (1992); **C58**, 199 (1993); **C61**, 1 (1994); Phys. Rep. **276**, 223 (1996).

BaBar: B. Aubert *et al.*: Phys. Rev. Lett. **87**, 162002 (2001); Phys. Rev. **D65**, 091104 (2002); Phys. Rev. **D75**, 012003 (2007); J.P. Lees *et al.*: Phys. Rev. **D88**, 032011 (2013).

Belle: K. Abe *et al.*, Phys. Rev. Lett. **88**, 052001 (2002); R. Seuster *et al.*, Phys. Rev. **D73**, 032002 (2006); M. Niijama *et al.*, `arXiv:1706.06791` .

CELLO: H.J. Behrend *et al.*: Z. Phys. **C46**, 397 (1990); **C47**, 1 (1990).

CLEO: S. Behrends *et al.*, Phys. Rev. **D31**, 2161 (1985); D. Bortoletto *et al.*, Phys. Rev. **D37**, 1719 (1988); erratum *ibid.* **D39**, 1471 (1989); and M. Artuso *et al.*, Phys. Rev. **D70**, 112001 (2004).

Crystal Ball: Ch. Bieler *et al.*, Z. Phys. **C49**, 225 (1991).

DELPHI: P. Abreu *et al.*: Z. Phys. **C57**, 181 (1993); **C59**, 533 (1993); **C61**, 407 (1994); **C65**, 587 (1995); **C67**, 543 (1995); **C68**, 353 (1995); **C73**, 61 (1996); Nucl. Phys. **B444**, 3 (1995); Phys. Lett. **B341**, 109 (1994); **B345**, 598 (1995); **B361**, 207 (1995); **B372**, 172 (1996); **B379**, 309 (1996); **B416**, 233 (1998); **B449**, 364 (1999); **B475**, 429 (2000); Eur. Phys. J. **C6**, 19 (1999); **C5**, 585 (1998); **C18**, 203 (2000); and J. Abdallah *et al.*, Phys. Lett. **B569**, 129 (2003); Phys. Lett. **B576**, 29 (2003); Eur. Phys. J. **C44**, 299 (2005); and W. Adam *et al.*: Z. Phys. **C69**, 561 (1996); **C70**, 371 (1996).

HRS: S. Abachi *et al.*, Phys. Rev. Lett. **57**, 1990 (1986); and M. Derrick *et al.*, Phys. Rev. **D35**, 2639 (1987).

L3: M. Acciarri *et al.*: Phys. Lett. **B328**, 223 (1994); **B345**, 589 (1995); **B371**, 126 (1996); **B371**, 137 (1996); **B393**, 465 (1997); **B404**, 390 (1997); **B407**, 351 (1997); **B407**, 389 (1997), erratum *ibid.* **B427**, 409 (1998); **B453**, 94 (1999); **B479**, 79 (2000).

MARK II: H. Schellman *et al.*, Phys. Rev. **D31**, 3013 (1985); and G. Wormser *et al.*, Phys. Rev. Lett. **61**, 1057 (1988).

JADE: W. Bartel *et al.*, Z. Phys. **C20**, 187 (1983); and D.D. Pietzl *et al.*, Z. Phys. **C46**, 1 (1990).

OPAL: R. Akers *et al.*: Z. Phys. **C63**, 181 (1994); **C66**, 555 (1995); **C67**, 389 (1995); **C68**, 1 (1995); and G. Alexander *et al.*: Phys. Lett. **B358**, 162 (1995); Z. Phys. **C70**, 197 (1996); **C72**, 1 (1996); **C72**, 191 (1996); **C73**, 569 (1997); **C73**, 587 (1997); Phys. Lett. **B370**, 185 (1996); and K. Ackerstaff *et al.*: Z. Phys. **C75**, 192 (1997); Phys. Lett. **B412**, 210 (1997); Eur. Phys. J. **C1**, 439 (1998); **C4**, 19 (1998); **C5**, 1 (1998); **C5**, 411 (1998); and G. Abbiendi *et al.*: Eur. Phys. J. **C16**, 185 (2000); **C17**, 373 (2000).

PLUTO: Ch. Berger *et al.*, Phys. Lett. **104B**, 79 (1981).

SLD: K. Abe, Phys. Rev. **D59**, 052001 (1999); Phys. Rev. **D69**, 072003 (2004).

TASSO: H. Aihara *et al.*, Z. Phys. **C27**, 27 (1985).

TPC: H. Aihara *et al.*, Phys. Rev. Lett. **53**, 2378 (1984).

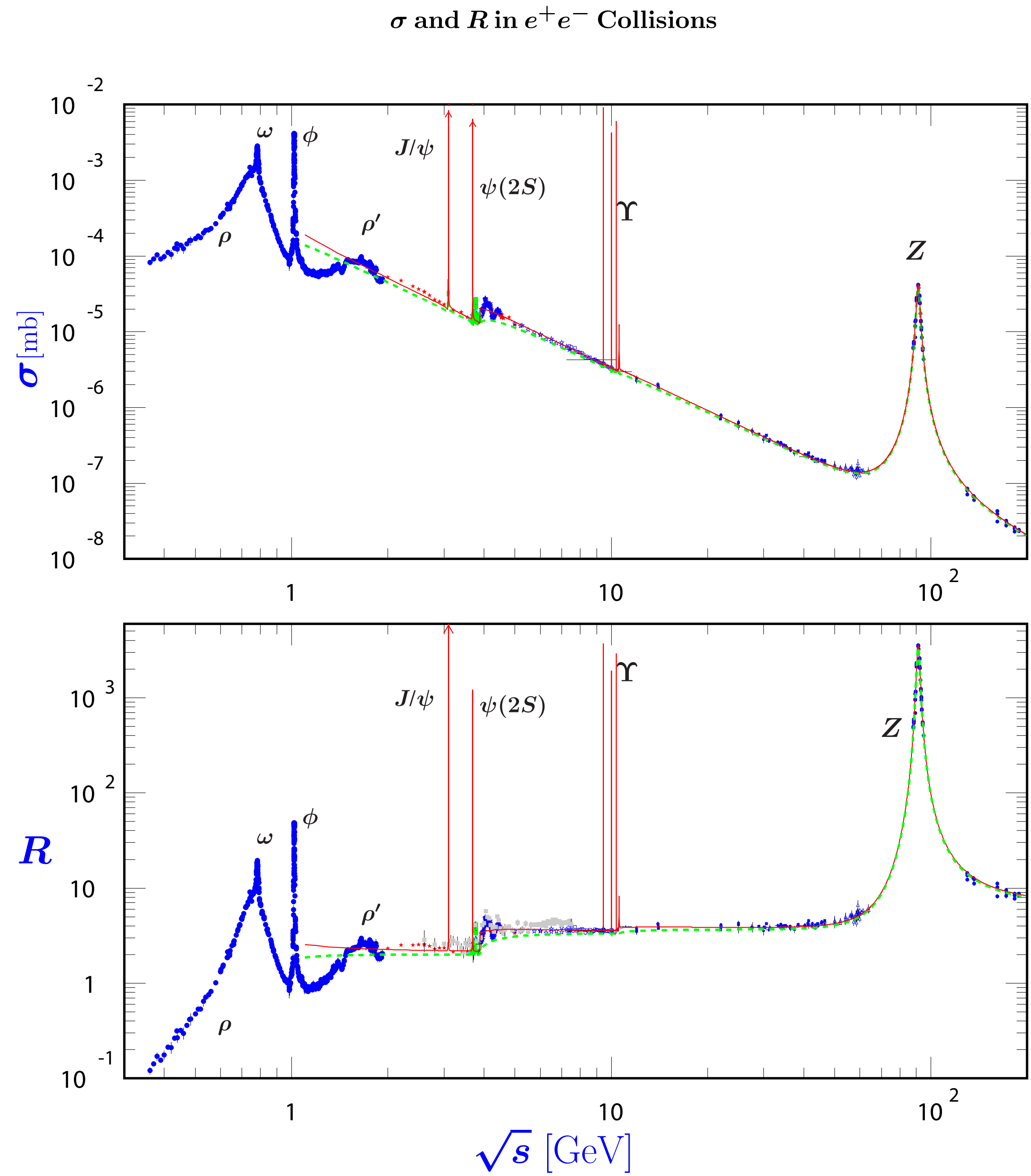

Figure 51.2: World data on the total cross section of $e^+e^- \rightarrow$ *hadrons* and the ratio $R(s) = \sigma(e^+e^- \rightarrow hadrons, s)/\sigma(e^+e^- \rightarrow \mu^+\mu^-, s)$. $\sigma(e^+e^- \rightarrow hadrons, s)$ is the experimental cross section corrected for initial state radiation and electron-positron vertex loops, $\sigma(e^+e^- \rightarrow \mu^+\mu^-, s) = 4\pi\alpha^2(s)/3s$. Data errors are total below 2 GeV and statistical above 2 GeV. The curves are an educative guide: the broken one (green) is a naive quark-parton model prediction, and the solid one (red) is 3-loop pQCD prediction (see "Quantum Chromodynamics" section of this *Review*, Eq. (9.7) or, for more details, K. G. Chetyrkin *et al.*, Nucl. Phys. **B586**, 56 (2000) (Erratum *ibid.* **B634**, 413 (2002)). Breit-Wigner parameterizations of J/ψ, $\psi(2S)$, and $\Upsilon(nS), n = 1, 2, 3, 4$ are also shown. The full list of references to the original data and the details of the R ratio extraction from them can be found in `[arXiv:hep-ph/0312114]`. Corresponding computer-readable data files are available at `http://pdg.lbl.gov/current/xsect/`. (Courtesy of the COMPAS (Protvino) and HEPDATA (Durham) Groups, August 2017. Corrections by P. Janot (CERN) and M. Schmitt (Northwestern U.))

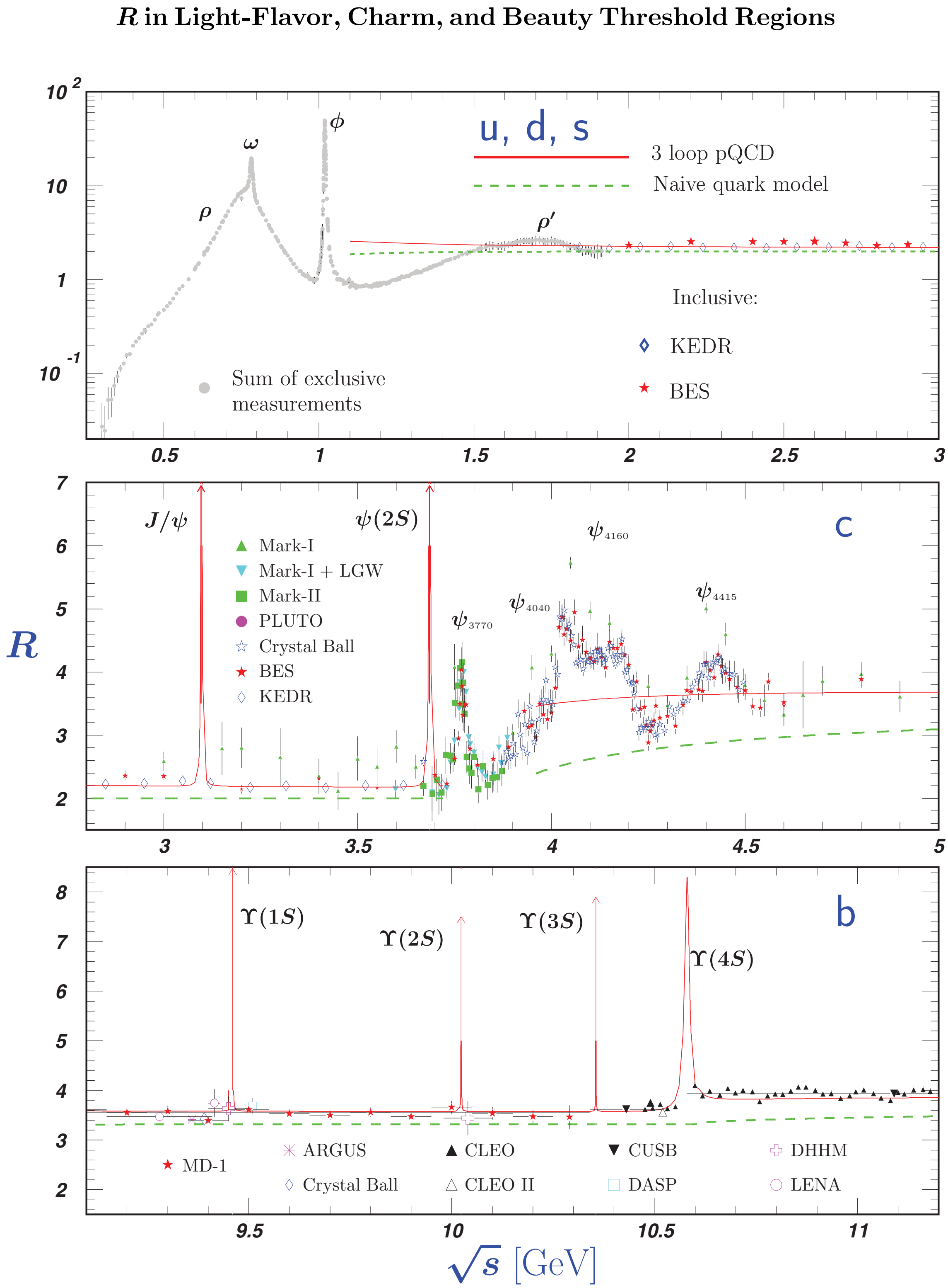

Figure 51.3: R in the light-flavor, charm, and beauty threshold regions. Data errors are total below 2 GeV and statistical above 2 GeV. The curves are the same as in Fig. 51.2. **Note:** CLEO data above $\Upsilon(4S)$ were not fully corrected for radiative effects, and we retain them on the plot only for illustrative purposes with a normalization factor of 0.8. The full list of references to the original data and the details of the R ratio extraction from them can be found in `[arXiv:hep-ph/0312114]`. The computer-readable data are available at `http://pdg.lbl.gov/current/xsect/`. (Courtesy of the COMPAS (Protvino) and HEPDATA (Durham) Groups, August 2017.)

Annihilation Cross Section Near M_Z

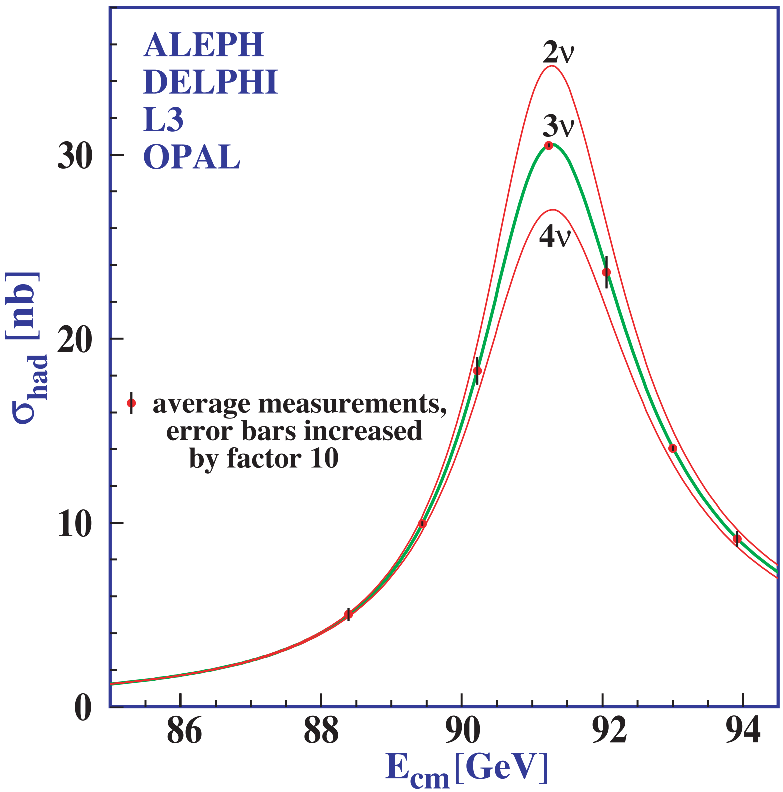

Figure 51.4: Combined data from the ALEPH, DELPHI, L3, and OPAL Collaborations for the cross section in e^+e^- annihilation into hadronic final states as a function of the center-of-mass energy near the Z pole. The curves show the predictions of the Standard Model with two, three, and four species of light neutrinos. The asymmetry of the curve is produced by initial-state radiation. Note that the error bars have been increased by a factor ten for display purposes. References:

ALEPH: R. Barate *et al.*, Eur. Phys. J. **C14**, 1 (2000).
DELPHI: P. Abreu *et al.*, Eur. Phys. J. **C16**, 371 (2000).
L3: M. Acciarri *et al.*, Eur. Phys. J. **C16**, 1 (2000).
OPAL: G. Abbiendi *et al.*, Eur. Phys. J. **C19**, 587 (2001).
Combination: The ALEPH, DELPHI, L3, OPAL, SLD Collaborations, the LEP Electroweak Working Group, and the SLD Electroweak and Heavy Flavor Groups, Phys. Rept. **427**, 257 (2006) `[arXiv:hep-ex/0509008]`.

(Courtesy of M. Grünewald and the LEP Electroweak Working Group, 2007)

Total Hadronic Cross Sections

(Updated August 2017, COMPAS group, IHEP, Protvino)

In this section, plots of total cross section for various processes are presented. The plots include data from hadronic collisions such as pp and $\overline{p}p$, as well as γp, γd, and $\gamma\gamma$ processes. The cross section data provide crucial inputs to the study of QCD physics. In particular, to probe the non-perturbative part of QCD processes which are described by a number of diffractive models. We begin by introducing some models of diffractive scatterings and listing references for further reading.

Diffractive scattering here means scattering of hadrons at small angles and exhibiting typical diffraction pattern in angular distribution of scattered particles. Beyond purely elastic scattering diffraction phenomena include inelastic processes with large rapidity gaps: those of single and double diffractive dissociation and "central diffractive" events. In distinction from the most of other processes considered in the SM diffraction processes (DP) are related to large spatio-temporal scales growing with energy of collision. Being caused by strong interactions DP are a subject of the fundamental strong interaction theory, QCD, and hereby a part of the longstanding problem of QCD at large distances.

One of the most important basic notions and tools in general theoretical framework related to the diffractive processes is the notion of the Regge poles, or Reggeons, generalizing the simple one-particle exchange (of Yukawa type) by virtual particles of fixed spin to exchanges by states with "running spin" dependent on the transferred momenta [1,2]. The simplest case of the one-Reggeon exchange amplitude is given by the amplitude (at high c.m. energy $\sqrt{s}$ and fixed (small) transferred momentum squared, t): $T(s,t) = \beta(t)s^{\alpha(t)}$ which qualitatively exhibits many typical features of generic diffractive processes (e.g. the growth of the interaction radius with energy). In practice the single-pole Reggeon model is insufficient for many diffractive processes but still serves a building block for more sophisticated schemes. Up to now no firm results concerning Regge trajectories $\alpha(t)$ and Regge residues $\beta(t)$ were obtained from the first principles of QCD. General principles imply that both $\alpha(t)$ and $\beta(t)$are analytic functions with right cuts from some $t_0 > 0$ to positive infinity.

The theoretical requisite for analyzing diffractive phenomena is therefore represented by various model approaches. The more commonly discussed models in the literatures are:

– **Regge -Eikonal approach** [3–10]: this approach automatically satisfy the s-channel unitarity condition and generalizes the impact parameter approximation to the relativistic case.

– **Regge pole models with minimal corrections due to two-Reggeon exchanges** [11–13]: in this model, contribution of the leading trajectory is supplemented by a two-Reggeon exchange with arbitrary coefficient chosen from the fitting details.

– ***U*-matrix (or resonance) approach** [14, 15]: the unitarity respecting approach with the scattering amplitude defined by a reaction matrix.

– **Direct functional modelling of the amplitudes without Regge trajectories** [16, 17]: this approach appeals to only very general properties of the amplitudes leaving aside all dynamical assumptions and mostly aiming at the best phenomenological description of the data.

– **Quasi-classical approach** [18–20]: based on the observation that diffractive processes deal with high quantum numbers, in particular with large number of virtual quanta.

For readers who are interested in examples of both total and elastic cross section parametrizations and fits, see previous edition of the *Plots of Cross Sections and Related Quantities* review [21]. For the cross section plots shown in the following pages, the example fits are using parametrizations as described in [21] with the fit range starting at about $\sqrt{s} = 5$ GeV.

References:

[1] P.D.B. Collins, *An Introduction to Regge Theory and High Energy Physics*, Cambridge: Cambridge University Press, 1977.
[2] G. Pancheri and Y. N. Srivastava, Eur. Phys. J. **C77**, 150 (2017).
[3] L. A. Harland-Lang, V. A. Khoze and M. G. Ryskin, Int. J. Mod. Phys. **A30**, 1542013 (2015).
[4] V. A. Petrov and A. Prokudin, Phys. Rev. **D87**, 036003 (2013).
[5] C. Bourrely, J. Soffer and T. T. Wu, Eur. Phys. J. **C28**, 97 (2003).
[6] M. M. Block, L. Durand, P. Ha and F. Halzen, Phys. Rev. **D92**, 014030 (2015).
[7] O. V. Selyugin, Phys. Rev. **D91**, 113003 (2015); Erratum: Phys. Rev. **D92**, 099901 (2015).
[8] L. G. Dakhno and V. A. Nikonov, Eur. Phys. J. **A5**, 209 (1999).
[9] A. A. Godizov, Phys. Lett. **B735**, 57 (2014).
[10] E. Gotsman, E. M. Levin and U. Maor, Phys. Rev. **D49**, R4321 (1994).
[11] A. Donnachie and P. V. Landshoff, Phys. Lett. **B727**, 500 (2013); Erratum: Phys. Lett. **B750**, 669 (2015).
[12] E. Martynov, Phys. Rev. **D87**, 114018 (2013).
[13] L. Jenkovszky, Nuovo Cim. C **037**, 99 (2014).
[14] S. M. Troshin and N. E. Tyurin, Int. J. Mod. Phys. **A32**, 1750103 (2017).
[15] V.V. Anisovich, Phys. Usp **58**, 10 (2015).
[16] D. A. Fagundes, M. J. Menon and P. V. R. G. Silva, Nucl. Phys. **A946**, 194 (2016).
[17] E. Martynov and B. Nicolescu, Eur. Phys. J. **C56**, 57 (2008).
[18] W. Heisenberg, Z. Phys. **133**, 65 (1952).
[19] V.V. Ezhela and Yu.P. Yushchenko, Preprint IHEP/IFVE-88-198 (1988).
[20] H. Nastase and J. Sonnenschein, Phys. Rev. **D92**, 105028 (2015).
[21] C. Patrignani *et al.* (Particle Data Group), Chin. Phys. C **40**, 100001 (2016) and 2017 update.

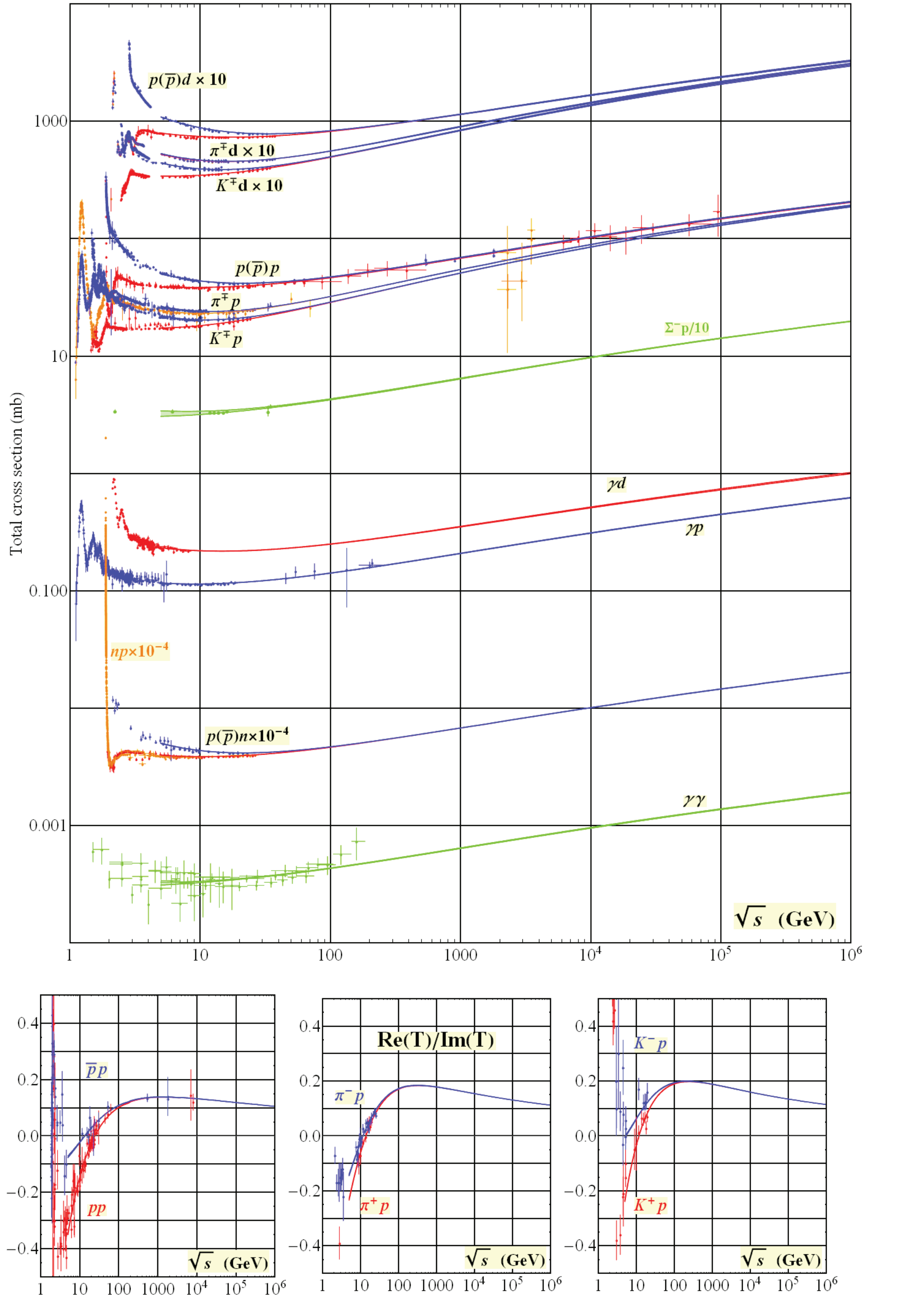

Figure 51.5: Summary of hadronic, γp, γd, and $\gamma\gamma$ total cross sections, and ratio of the real to imaginary parts of the forward hadronic amplitudes (T). Corresponding computer-readable data files may be found at `http://pdg.lbl.gov/current/xsect/`. (Courtesy of the COMPAS group, IHEP, Protvino, August 2017.)

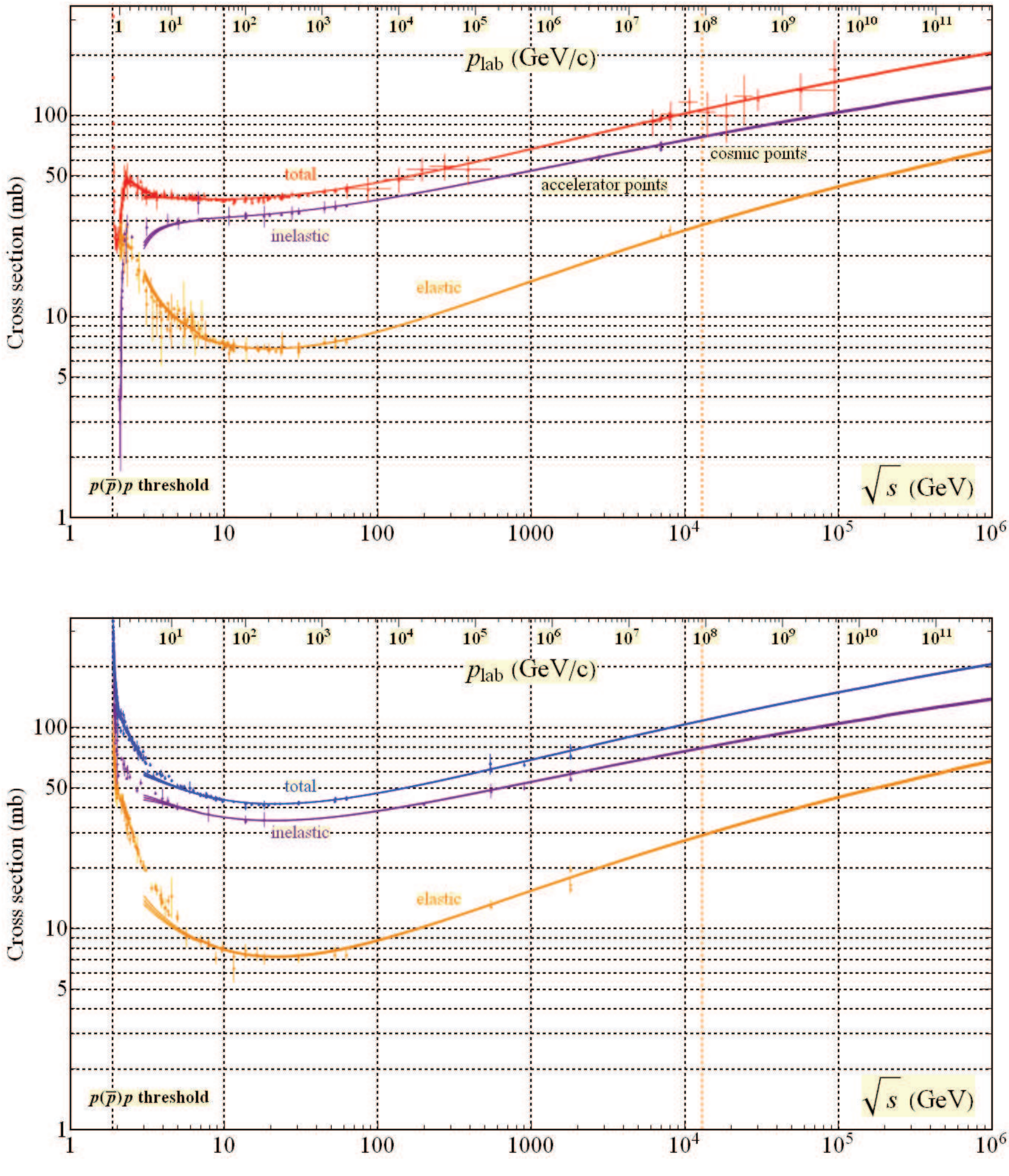

Figure 51.6: Total and elastic cross sections for pp and $\overline{p}p$ collisions as a function of laboratory beam momentum and total center-of-mass energy. Corresponding computer-readable data files may be found at `http://pdg.lbl.gov/current/xsect/`. (Courtesy of the COMPAS group, IHEP, Protvino, August 2017)

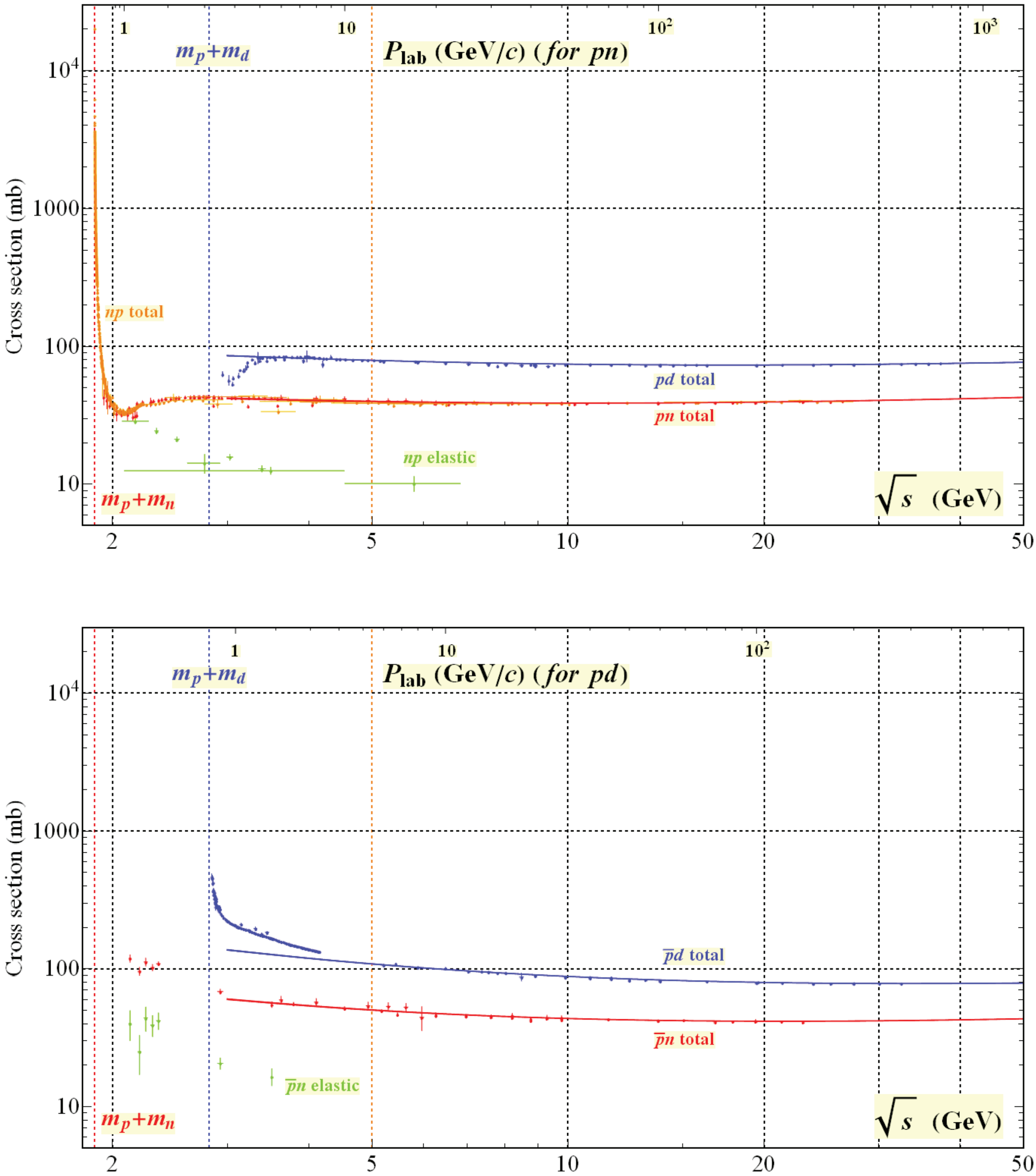

Figure 51.7: Total and elastic cross sections for pd (total only), np, $\overline{p}d$ (total only), and $\overline{p}n$ collisions as a function of laboratory beam momentum and total center-of-mass energy. Corresponding computer-readable data files may be found at `http://pdg.lbl.gov/current/xsect/`. (Courtesy of the COMPAS Group, IHEP, Protvino, August 2017)

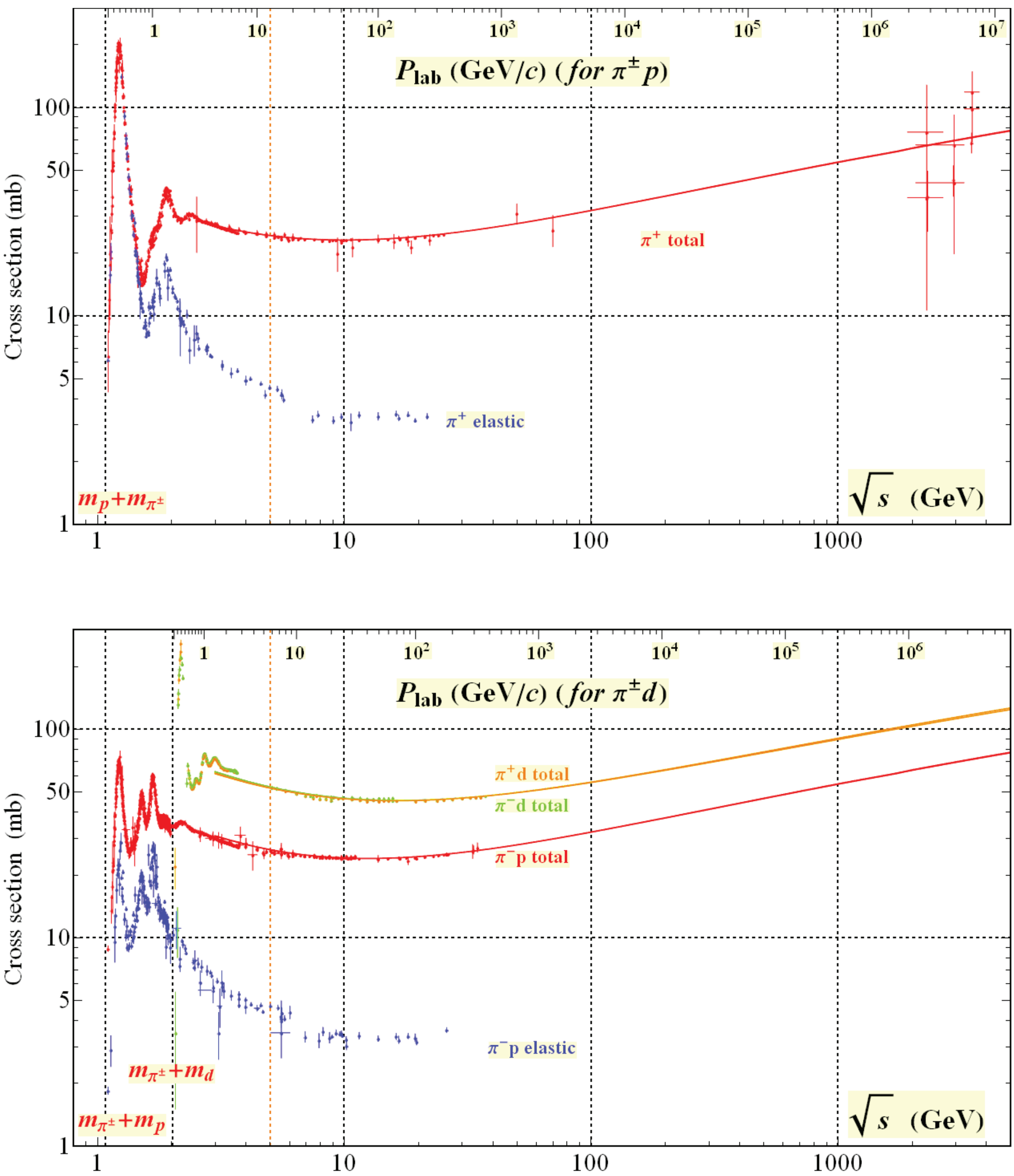

Figure 51.8: Total and elastic cross sections for $\pi^{\pm}p$ and $\pi^{\pm}d$ (total only) collisions as a function of laboratory beam momentum and total center-of-mass energy. Corresponding computer-readable data files may be found at `http://pdg.lbl.gov/current/xsect/`. (Courtesy of the COMPAS Group, IHEP, Protvino, August 2017)

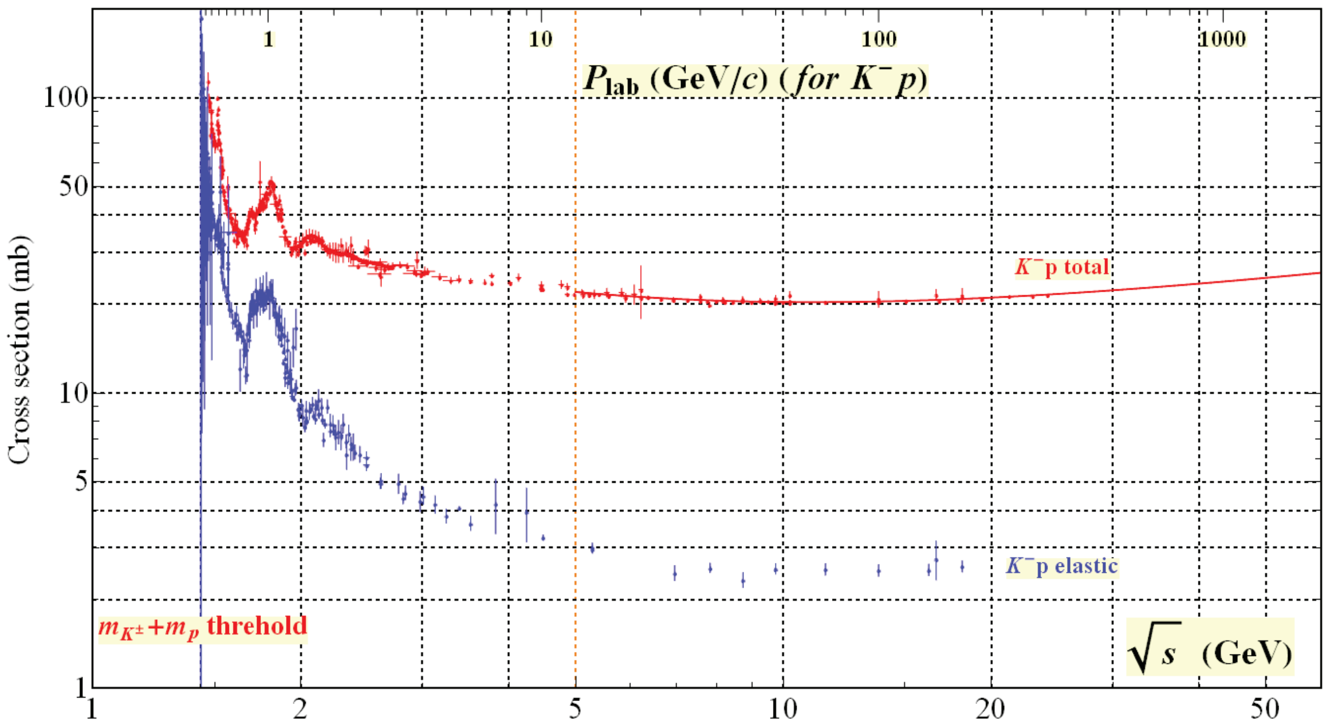

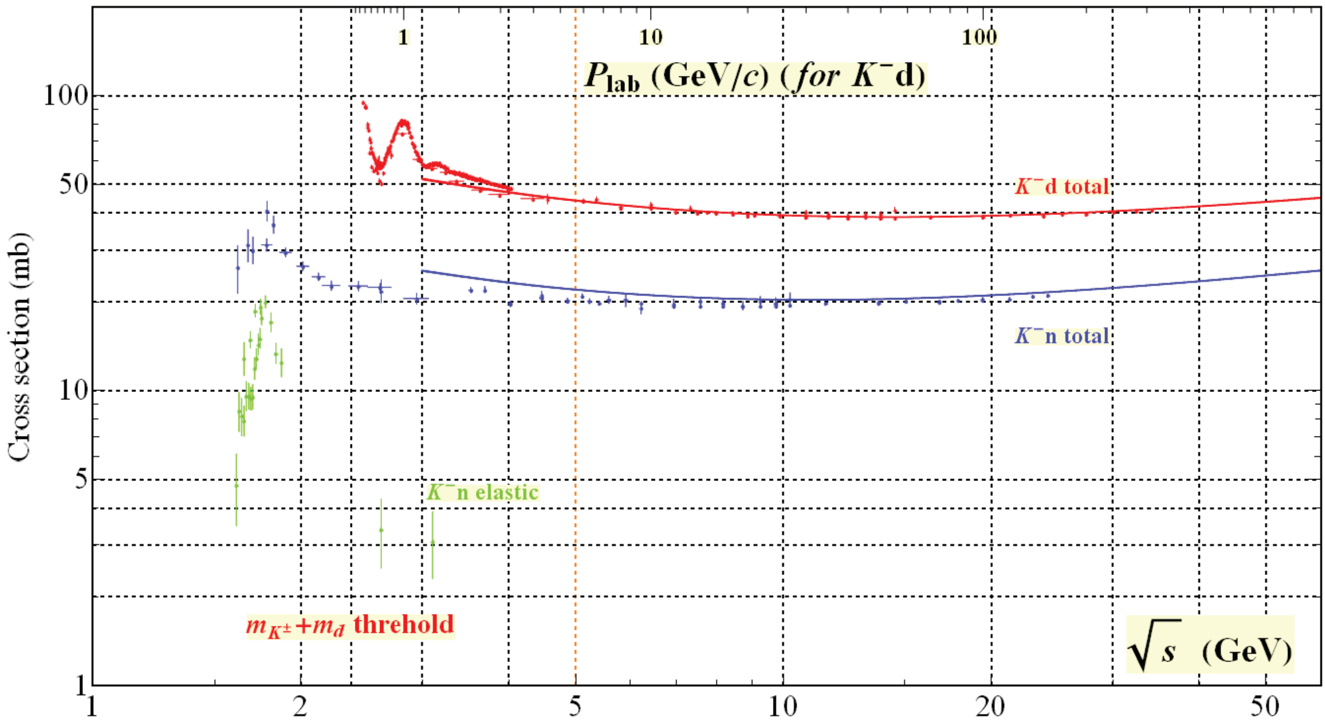

Figure 51.9: Total and elastic cross sections for K^-p and K^-d (total only), and K^-n collisions as a function of laboratory beam momentum and total center-of-mass energy. Corresponding computer-readable data files may be found at `http://pdg.lbl.gov/current/xsect/`. (Courtesy of the COMPAS Group, IHEP, Protvino, August 2017)

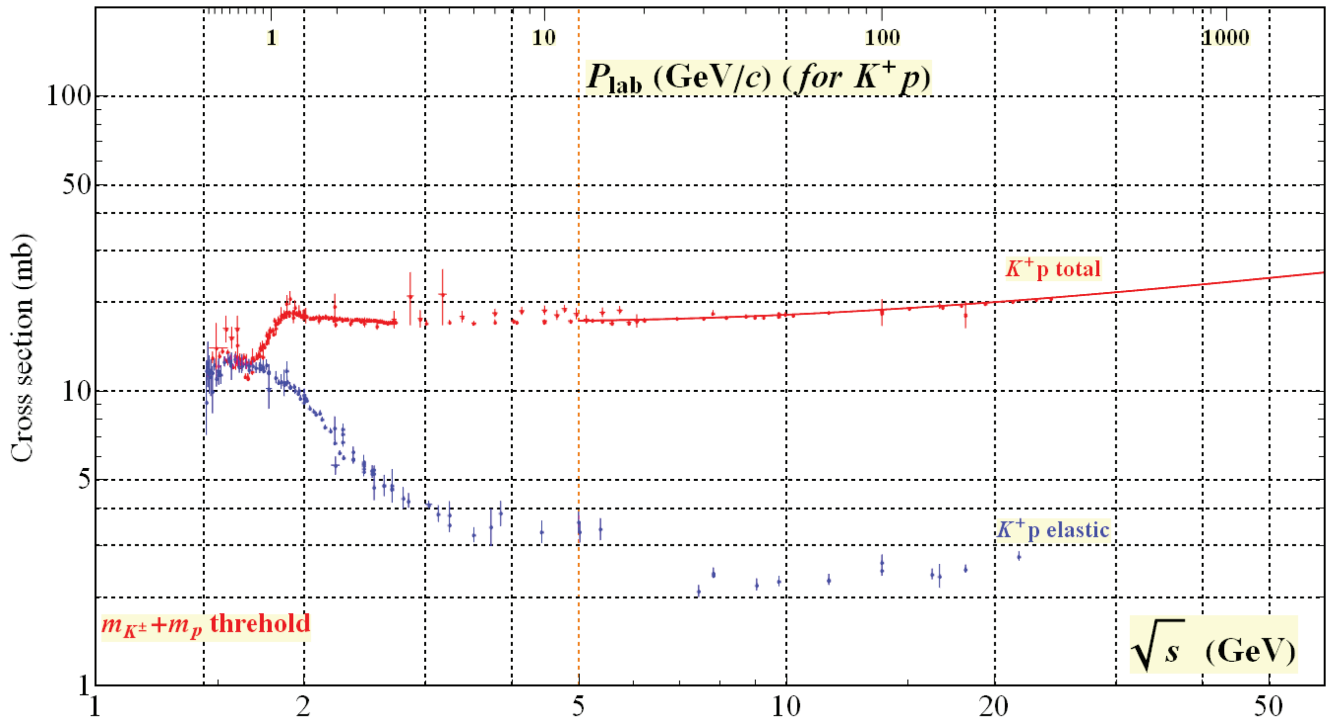

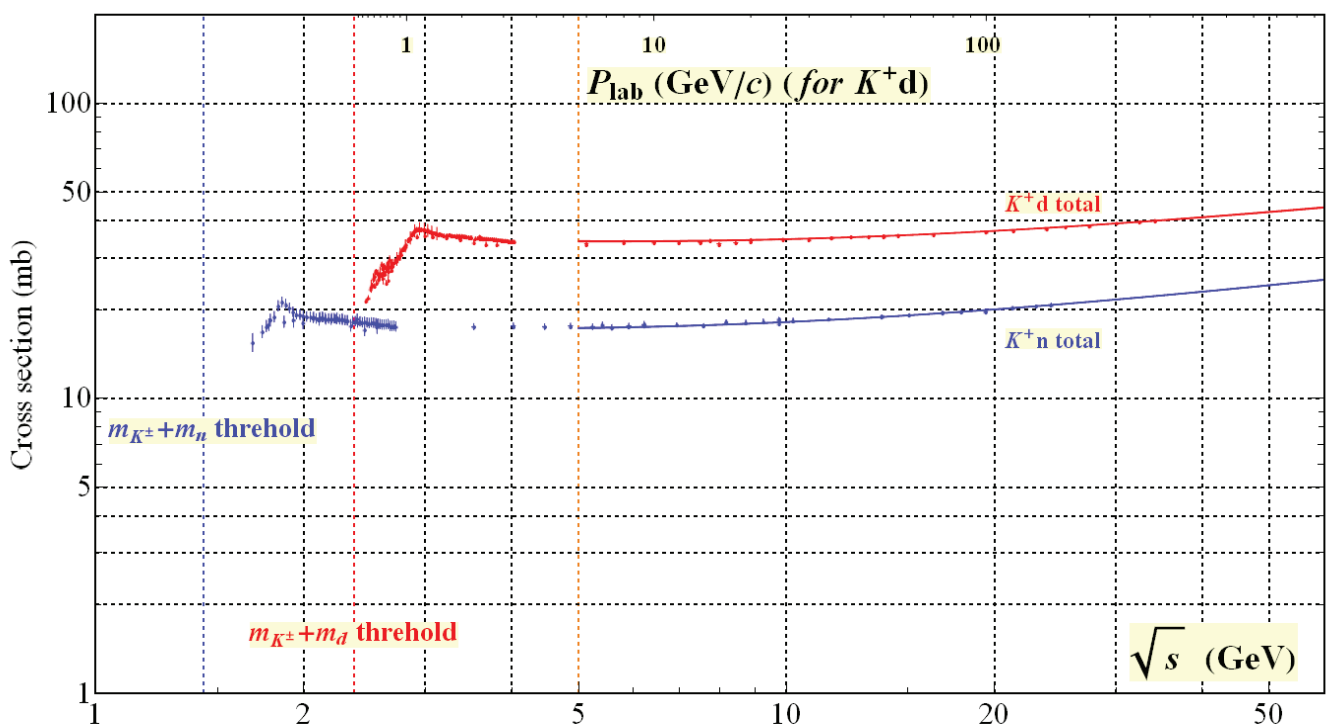

Figure 51.10: Total and elastic cross sections for K^+p and total cross sections for K^+d and K^+n collisions as a function of laboratory beam momentum and total center-of-mass energy. Corresponding computer-readable data files may be found at `http://pdg.lbl.gov/current/xsect/`. (Courtesy of the COMPAS Group, IHEP, Protvino, August 2017)

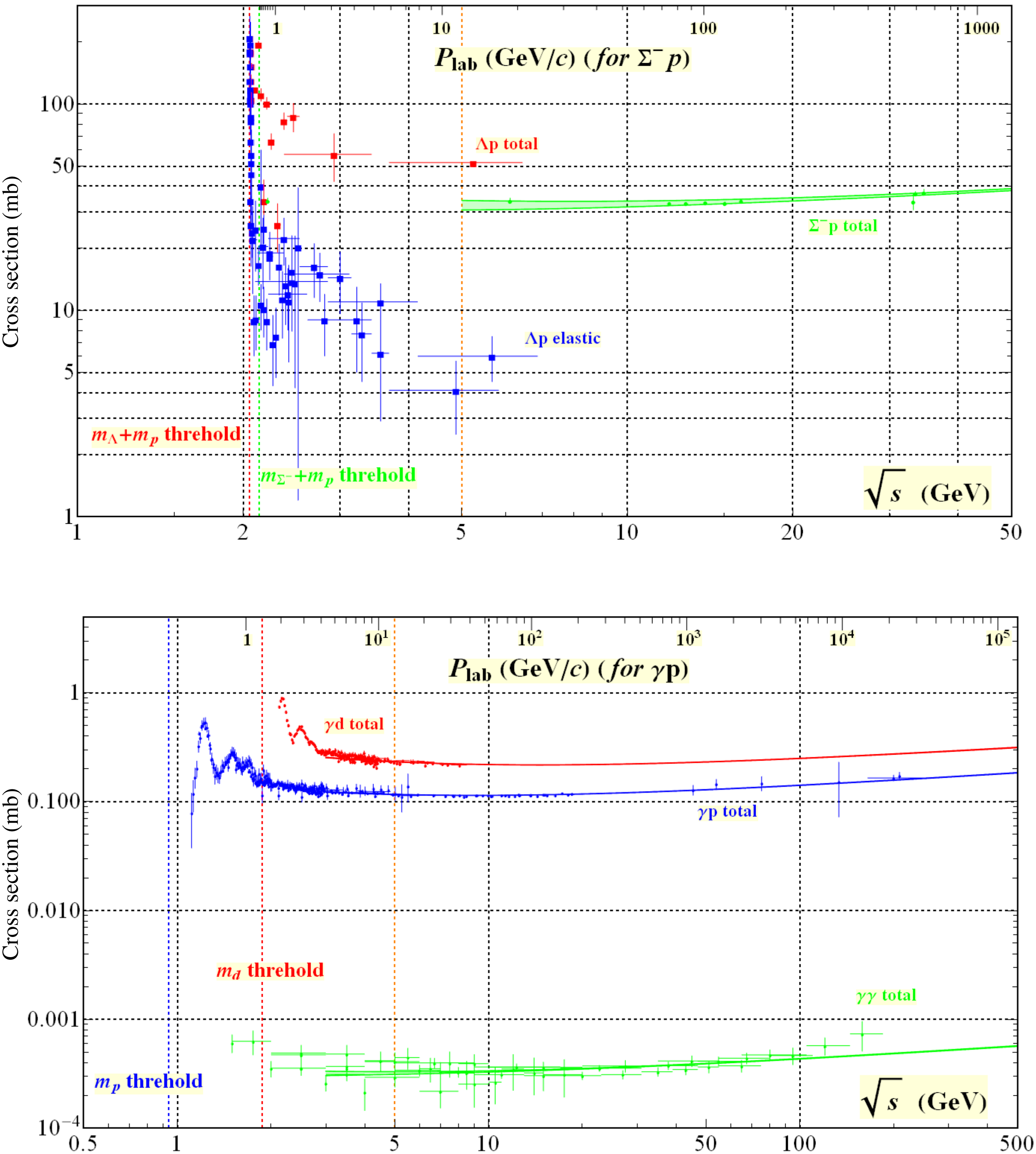

Figure 51.11: Total and elastic cross sections for Λp, total cross section for $\Sigma^- p$, and total hadronic cross sections for γd, γp, and $\gamma\gamma$ collisions as a function of laboratory beam momentum and the total center-of-mass energy. Corresponding computer-readable data files may be found at `http://pdg.lbl.gov/current/xsect/`. (Courtesy of the COMPAS group, IHEP, Protvino, August 2017)